Two-Phase Flow Behavior in the Freeboard of a Gas-Fluidized Bed

An experimental and theoretical study was conducted to identify the flow behavior of gas and particulates in the freeboard of a gas-fluidized bed. The axial velocity and turbulence intensity distributions were measured along the centerline and across the freeboard. A laser Doppler velocimeter (LDV) was used for the experiments. A technique based on fluorescence emission was developed to discriminate between gas-phase and particle-phase velocity information. The gas phase measurements revealed a strong influence of bubble induced turbulence on gas velocity distribution. The axial particle velocity indicated a two-stage decay with height. Models were developed to predict centerline gas velocity and transport disengagement height.

F. Hamdullahpur, and G. D. M. MacKay
Department of Chemical Engineering
and Center for Energy Studies
Technical University of Nova Scotia
Halifax, Nova Scotia, Canada

Introduction

In fluidized-bed combustion (FBC) of solid fuels, elutriation of fuel and incomplete combustion lead to lower combustion efficiency and high emissions. To overcome this deficiency requires better knowledge of the behavior of the freeboard region of a gas-solid fluidized bed.

Although it is recognized that particle movement and chemical reactions in the freeboard depend strongly on the air flow field, only limited information is available on the real behavior of the two-phase flow. Most efforts have concentrated on the measurement of global freeboard properties such as solids holdup and entrainment rate. Information on the velocity distribution of the two phases is essential to gain a thorough understanding of the flow behavior in the freeboard of FBC, to test and improve flow models, and to reliably predict the transport disengagement height (TDH).

In this investigation, the local mean and RMS velocities of the gas and particles were measured using a laser-fluorescence doppler velocimeter to map the two-phase flow distribution in the freeboard.

The results obtained from the two-phase flow measurements bring new information to the understanding of freeboard phenomena. The gas phase measurements show a fast decay of gas, local mean, and RMS velocity profiles with freeboard height. The freeboard gas flow is strongly influenced by distribution of the erupting bubbles at the bed surface. The horizontal gas velocity profiles reveal that close to the bed surface the maximum velocity is located at the column center; this is attributed to the migration of bubbles toward the symmetry axis in the dense bed (Grace and Harrison, 1968; Al Taweel and Landau, 1978). At greater freeboard height, the location of the maximum velocity shifts toward the column wall. This kind of velocity distribution supports the concept of so-called ghost bubbles in the freeboard (see the Theoretical section in Results, below) (Kehoe, 1969; Pemberton and Davidson, 1984). From experiments at different bed depths, it was found that the turbulence intensity increases with bubble diameter.

The axial particle velocity measurements indicate a two-stage decay of the velocity profile with freeboard height. The shape of the velocity profile changes abruptly when the local mean particle velocity becomes equal to the superficial gas velocity; this behavior has never been reported in the literature. A simple model was developed to predict the gas velocity along the freeboard axis. The turbulent decay coefficient, $\beta = 1/3\ D_b$, derived from the model agrees reasonably well with the experimental gas velocity and also explains the experimental findings of Pemberton and Davidson (1984) and Horio et al. (1980). The expression for transport disengagement height, $TDH = 12\ D_b$, is also derived from the model; it predicts the TDH within 5% of the experimental values.

Flow behavior in the region between the bubbling bed and the TDH is very complex; it cannot be predicted by bulk duct flow assumptions. This work shows that freeboard gas flow is strongly influenced by the distribution of bubbles erupting at the bed surface. The results support the concept of ghost bubbles in the freeboard. With the information obtained from the experiments, two models are proposed: one to predict the gas velocity along the freeboard axis, and one to predict the TDH.

Correspondence concerning this paper should be addressed to F. Hamdullahpur.

Table 1. Previous Particle and Gas Velocity Measurements in Freeboard

Researchers	Measurement Technique: Gas	Measurement Technique: Particle	Particle Type, Size	Bed Size	$\bar{U}$ m/s
Do et al. (1972)	—	Fast photography	Glass beads 177–250 μm	56 × 1 cm	0.4
Fournol et al. (1973)	Hot wire	—	FCC 58 μm	60 cm	0.11–0.22
Morooka et al. (1980)	—	Fiber optics	60 μm	0.066; 0.12 m	0.5–2.5
Horio et al. (1980)	Hot wire	Fiber optics	Glass beads 0.164–1.35 mm	0.24 cm	0.3–0.6
Levy & Lockwood (1983)	LDV	LDV	Sand 0.4–1.0 mm	610 × 305 mm	0.2–1.1
Pemberton & Davidson (1984)	Hot wire	—	Polymer 760 μm; sand 370 μm	0.6 m; 0.3 × 0.3 m	0.2–0.5

LDV: Laser Doppler velocimetery.

Experimental

Previous work

A good understanding of the two-phase flow behavior above the bubbling bed surface and in the freeboard is essential to the study of particle migration from the bed. Because of the complexity of two-phase flow, most efforts have concentrated on measurement of global freeboard properties such as solids holdup and entrainment rate. Some workers, however, measured particle and/or gas phase velocity distributions in the freeboard, as listed in Table 1.

Horio et al. (1980) used a fiber optic probe and a hot wire anemometer to measure particle and gas velocities, respectively. They reported that turbulence intensity in the freeboard increases with increasing gas velocity and bed depth, and with decreasing particle size. Turbulence intensity values in the freeboard between 5 and 40% were reported. Morooka et al. (1983) used a fiber optic probe and a thermal response probe to identify the flow patterns of 66 μm dia. solid particles. They concluded that below the TDH, the solids recirculate in the freeboard with a rate much higher than the net entrainment area. They did not measure the gas velocity or turbulent fluctuations. Levy and Lockwood (1983) were the first to use a nonintrusive technique to measure the gas velocity and the particle velocity fields in the freeboard simultaneously. They used a 5 mW helium-neon based laser Doppler velocimeter with a pedestal amplitude detection facility to discriminate gas and particle velocities. They presented the variation of gas velocity across the freeboard at various heights and superficial gas velocities. Their mean gas velocity profile exhibits a maximum near the wall and a minimum on the column centerline. The variation of axial gas velocity along the centerline and across the freeboard shows that both the centerline velocity and the horizontal velocity profiles are constant with freeboard height. This does not reflect the effect of turbulent energy dissipation with freeboard height on the gas velocity field. In the gas phase velocity measurements, Levy and Lockwood assumed the velocity of fine particles, generated by attrition of the bed material, to be the gas phase velocity; the air flow was not seeded. In a bed of 1 mm particles, however, continuous generation of 1 μm size particles by attrition is implausible. Pemberton and Davidson (1984) recently measured the turbulence in the freeboard of a 0.6 m dia. bed of 760 μm polymer particles and a 0.3 m square bed of 370 μm sand particles; a hot wire anemometer was used for measurements. They concluded that above the bed surface, the turbulence decays to the level characteristic of flow at the fluidizing velocity in the empty tube containing the bed.

With the exception of Levy and Lockwood, all the workers mentioned used a hot wire anemometer or an optical fiber probe. Both techniques are intrusive; the disturbance of the flow field can result in inaccurate measurement. Using a hot wire anemometer for gas velocity measurements while the solids are present is not appropriate because of the impingement of solids upon the wire.

Experimental setup

A cold fluidized bed, 319 mm × 176 mm rectangular cross section, was used. The column was constructed such that sections could be added to vary the height of the unit, as shown in Figure 1. The total height above the distributor plate was 4 m. The column was made of a 7 mm Plexiglas. First-quality crown glass plates were mounted on one column section to ensure good optical access; this section was interchanged with other sections when measurements were made in other freeboard locations.

The fluidizing air was supplied, at atmospheric pressure and room temperature, by a 2½ in. (6.35 cm) variable speed furnace blower. The air flow rate was measured by a 1¼ in. (3.18 cm) orifice plate. A humidifier box was used to minimize the static charge buildup on the column walls.

The air distributor was a 5 mm thick porous aluminum plate with 209 holes of 2.9 mm dia. Sand particles of 300 μm mean dia. (group B particles in Geldart's classification) were used as the bed material.

Measurement technique

An argon-ion based (green light at $\lambda = 514.5$ nm), single-channel, on-axis backscatter laser Doppler velocimeter system (TSI model 9100) was used. The LDV system can measure the sand particle velocity directly; seeding is not required. For gas velocity measurements, however, the air flow must be seeded to obtain velocity information. A fluidized-bed seeding generator was designed. Alumina oxide particles not larger than 1 μm dia. were elutriated from the generator (Amyotte and Hamdullahpur, 1984). The presence of seed particles in the freeboard together with sand particles complicates the measurement since both scatter light and yield velocity information. Unless one can simultaneously measure velocity and particle size, it is not possible to distinguish from which particle group the velocity information comes.

A nonintrusive technique was developed to overcome this deficiency (Hamdullahpur, 1985). The basic principle of the technique is optical discrimination between the scattered light and fluorescence emission from coated particles. To distinguish the velocity information from different particle groups, the seed particles were impregnated with Rhodamine 6G fluorescent dye

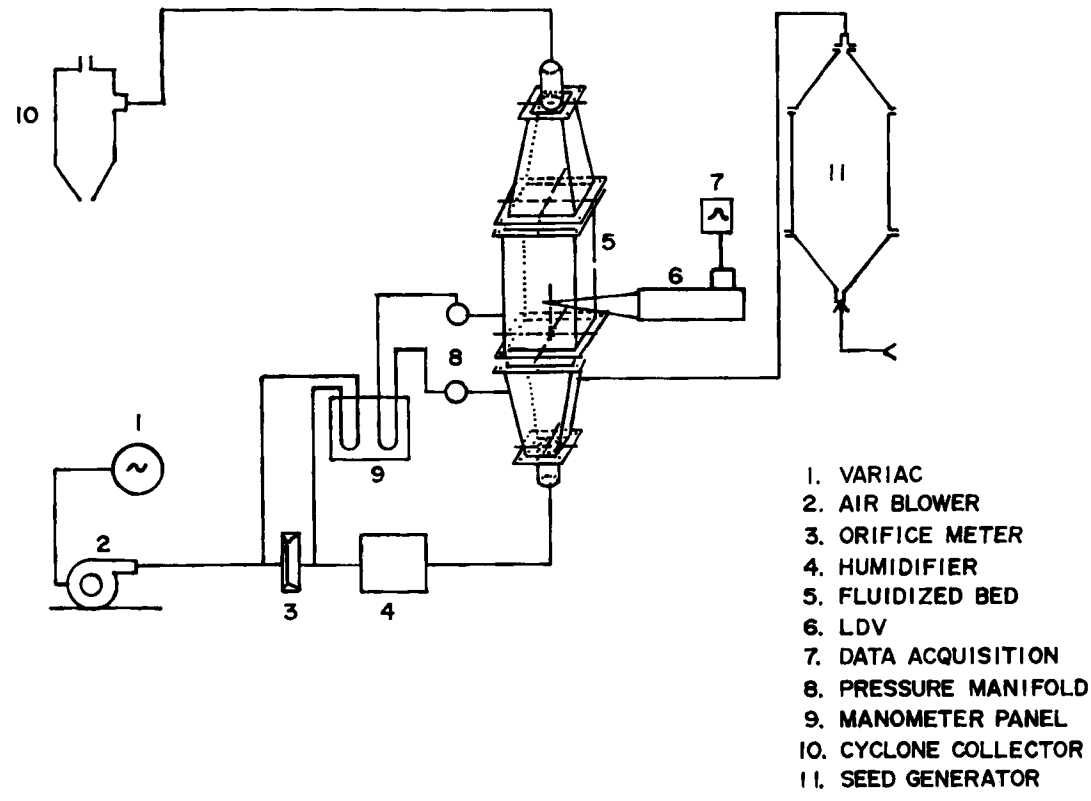

Figure 1. Diagram of experimental setup.

solution. The fluorescence emission from the Rhodamine 6G is at wavelengths longer than the argon-ion laser wavelength (Parker, 1968; Stevenson et al., 1975); this is shown in Figure 2. The scattered light from the undyed particles is eliminated by placing an optical narrow bandpass filter (Optikon FS10-25) with a central wavelength of 560 nm (orange) between the receiving assembly and photodetector pinhole.

By this technique, the velocity information is detected from only one group of particles although the other group is present in the flow; the details of the technique can be found elsewhere (Hamdullahpur, 1985).

The scattered light from particles is received into a counter-type signal processor (TSI model 1980). The signal processor is interfaced with an IBM PC microcomputer for subsequent data handling. A 0.5 MHz frequency shift value was selected to detect velocities in the direction opposite to the mean flow. Software was written to process the data and compute the mean velocity, standard deviation of the fluctuation (RMS), and a velocity histogram. After each velocity measurement, the information is displayed on the monitor screen and printed if desired.

The system was mounted on a vibration-free optical bench because the alignment of the optical components of the LDV system is very sensitive to vibration. Since the optical system could not move, the experimental rig was moved in the x-y-z direction to enable measurements at different locations in the freeboard. The traversing table is designed to move 130 cm in the z direction and 50 and 30 cm in the y and x directions, respectively.

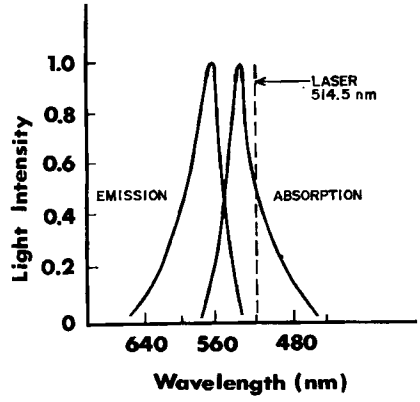

Figure 2. Adsorption and emission spectrum of Rhodamine 6G (Parker, 1968).

Results

A series of experiments was conducted to investigate two-phase behavior in the freeboard. The experiments were performed for six different fluidizing velocities at two bed heights. At each fluidizing velocity, the sand particle velocity, the gas phase velocity, and their RMS velocities were measured. In the experiments, the fluidizing velocities were much smaller than the terminal velocity of sand particles; thus, no sand particles were carried out from the freeboard. At each measurement location 1,000 to 3,000 data points were collected to obtain mean and RMS velocity values. Measurements in the immediate vicinity of the bed surface and at very large distances above the bed (only for sand particles) were not possible because of very

Table 2. Experimental Program

Fluidizing Velocity ms^{-1}	Static Bed Depth cm	Particle Mean Dia. μm	Exp. Group	
0.12	5.2	300 sand	Gas and solids	SG1
0.20	5.2	300 sand	Gas and solids	SG2
0.20	12	300 sand	Gas only	G2
0.28	5.2	300 sand	Gas and solids	SG3
0.28	12	300 sand	Gas only	G3
0.40	5.2	300 sand	Gas and solids	SG4
0.40	12	—	Gas only	G4
0.45	5.2	—	Gas and solids	SG5
0.60	5.2	—	Gas and solids	SG6

high and very low sand particle concentrations, respectively. The experimental program is given in Table 2.

Figure 3 shows the variation of gas phase local mean velocities with freeboard height along the column centerline ($x = 0$, $y = 0$) for six different fluidizing velocities. Turbulent fluctuation velocities (RMS) are also shown. The gas phase velocity decays with height and becomes constant at the superficial gas velocity. Although the centerline velocity decreases with freeboard height, this is compensated by the increase of the gas phase velocity away from the centerline (see Figure 7). Thus, the volumetric average gas phase velocity over the freeboard cross section remains constant, preserving the conservation of air mass flow rate. The RMS fluctuation velocity follows a similar decay pattern and reaches a constant value at about the freeboard height where the local mean gas velocity reaches the superficial gas velocity. Levy and Lockwood (1983) reported that the axial mean gas velocity was constant. This is probably because they did not seed the air flow in the LDV measurements; the particles were too coarse to follow the gas fluctuations.

The particle phase (sand) local mean velocity distribution in the positive z direction (i.e., rising particle) exhibits a different kind of variation with freeboard height, Figure 4. Up to a certain freeboard height above the bed surface the sand velocity is greater than the superficial gas velocity. At this point the shape

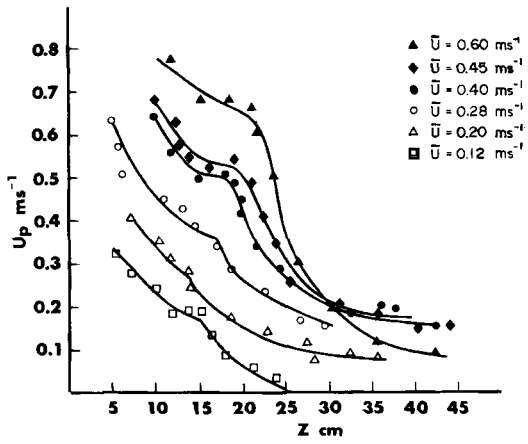

Figure 4. Variation of axial particle velocities (dp = 300 μm) with freeboard height at column centerline ($x = 0$, $y = 0$).
Bed depth, H = 5.2 cm.

of the distribution changes abruptly and the velocity decays more rapidly. This behavior of the particulate phase has not been reported in the literature. A possible explanation for this kind of sand velocity profile is that the particles are ejected with the ghost bubbles at their initial rising velocities. After leaving the bed surface, the particles decelerate along with the ghost bubbles until the ghost bubble relative velocity is the same as the average gas velocity, Figure 5. At that stage, particles disengage from the ghost bubble and pursue trajectories dictated by gravitational and drag forces. The low concentration of particles prevented measurements at higher freeboard levels.

Results of particle velocity measurements by horizontal traversing at several freeboard heights for fluidizing velocity $\bar{U}$ = 0.45 ms^{-1} are presented in Figure 6.

The mean values for sand particle velocities show no significant variation with horizontal location in the central ascending zone. A slight influence of the high gas velocity near the wall for $\bar{U}$ = 0.45 ms^{-1} can be observed in Figure 5 ($x = 0$, $y = 13$ cm, $z = 16$ cm). At lower $\bar{U}$ values this influence is not observed. It is also seen that at $z = 16$ cm freeboard height the rising particle

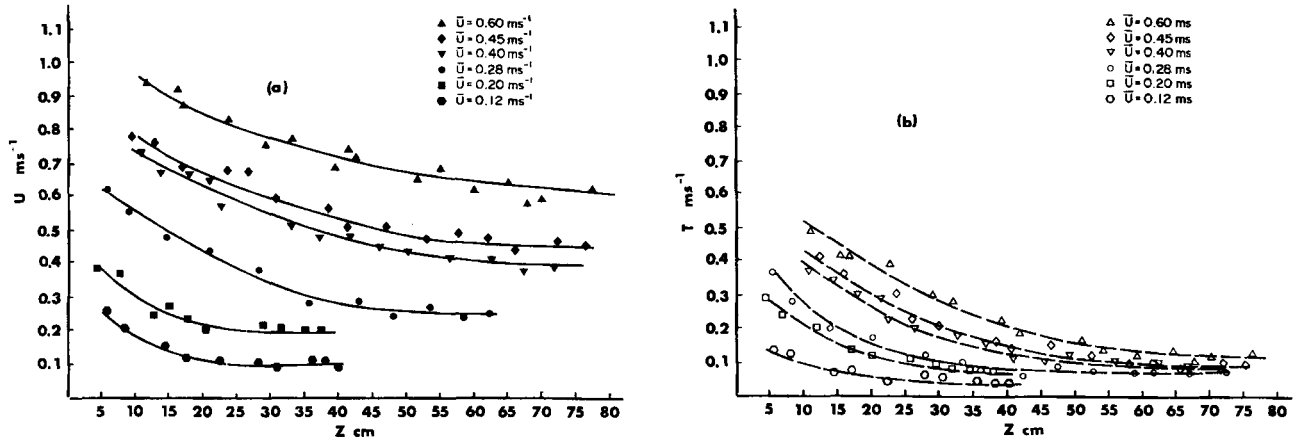

Figure 3. Variation of axial local mean and RMS gas velocities with freeboard height at column centerline ($x = 0$, $y = 0$).
Bed depth, H = 5.2 cm.

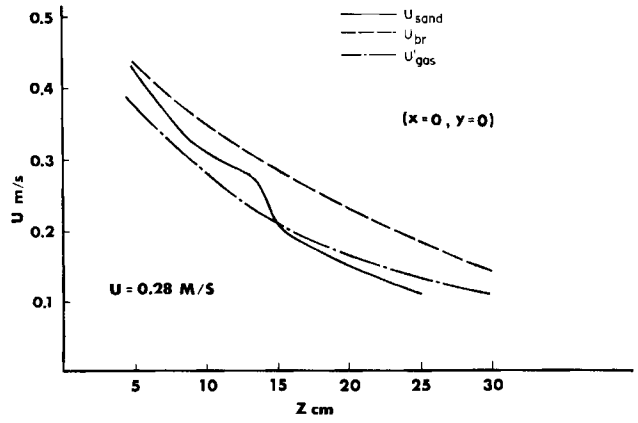

Figure 5. Comparison of axial sand velocity with relative ghost bubble velocity and gas RMS velocity.

velocity is 2.6 times greater than the falling particle velocity. At $z = 20$ (after the critical height, see Figure 4) they become nearly equal, indicating the dominant effect of gas velocity on particle movement in this region.

Although no attempt was made to obtain a quantitative expression for the wall zone thickness, its effect can be seen on particle velocities entering the wall zone. These particles (i.e., rising particles) move much slower than the particles in the central zone, and eventually fall back onto the bed surface.

Horio et al. (1980) postulated the existence of the wall zone and suggested that its thickness decreases exponentially with freeboard height. The experimental observations confirm this suggestion. Lateral particle velocity measurements by Morooko et al. (1983) show similar behavior.

The mechanism whereby the sharp change in the axial sand velocity profile occurs is not completely understood and requires further investigation. Figure 7 shows the variation of gas velocity across the freeboard at several heights for two fluidization velocities. For $\bar{U} = 0.20$ ms^{-1} (Figure 7a), at $z = 7.4$ cm above the bed surface the gas velocity shows a symmetrical but irregular variation. The maximum velocity is located at the symmetry axis (centerline) and has a value of 0.35 ms^{-1}, substantially larger than the fluidizing velocity. The velocity profiles show a rapid decrease from the centerline to a broad plateau and then another sharp decrease near the wall. The presence of a slow-moving gas zone near the wall can be seen from the figure. Measurements close to the wall at this height are not possible because of column vibration. By extrapolating the profile, the location of the zero gas velocity is found at about $y = 11$ cm. At distances greater than 11 cm the flow changes its direction and moves downward. At $z = 12.5$ cm ($x = 0$) above the bed surface the velocity profile takes an entirely different shape; it has a minimum at the center and peak values near the walls. It is also seen that the thickness of the wall zone decreases at this height. At $z = 15$ cm the same type of behavior is observed but at $z = 30$ cm the velocity distribution takes a more familiar form, as in the flow of air in a duct. It is clearly seen that the effect of bubble-induced turbulence has diminished at this height and the air has reached the fully developed flow region. It is assumed that above this height the gas velocity profile is independent of height and maintains its shape to the exit.

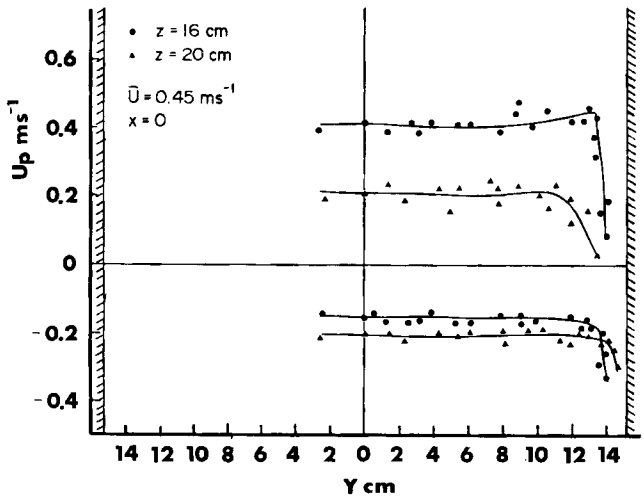

Figure 6. Horizontal distribution of rising and falling particle velocities ($dp = 300$ μm) along y axis ($x = 0$).
Bed depth, $H = 5.2$ cm.

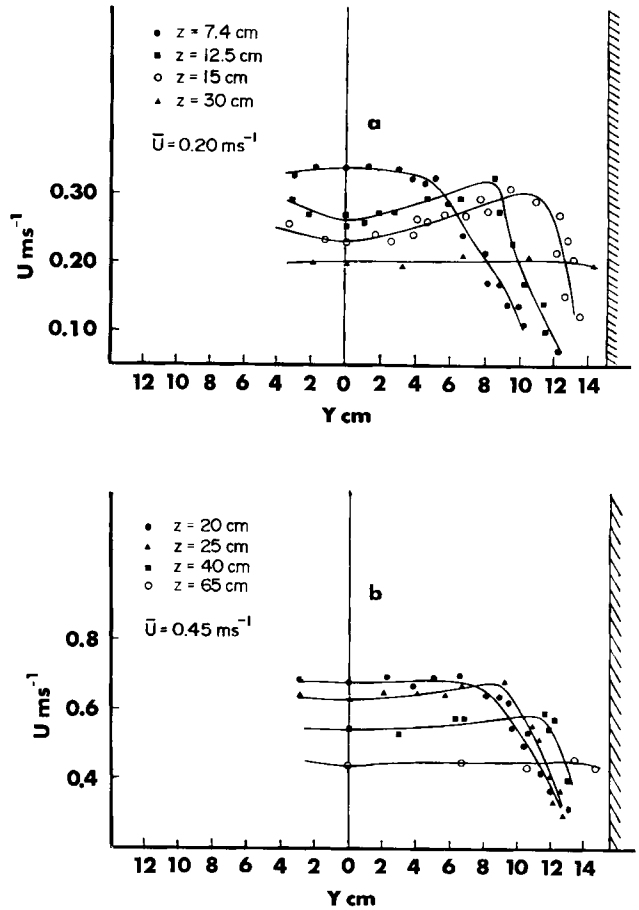

Figure 7. Horizontal distribution of local mean gas velocities along y axis ($x = 0$).
Bed depth, $H = 5.2$ cm.

The lateral turbulence intensity variations of the gas velocity at four different freeboard levels are shown in Figure 8. The turbulence intensity increases with distance from the centerline and, after reaching a maximum level, decays to the free stream

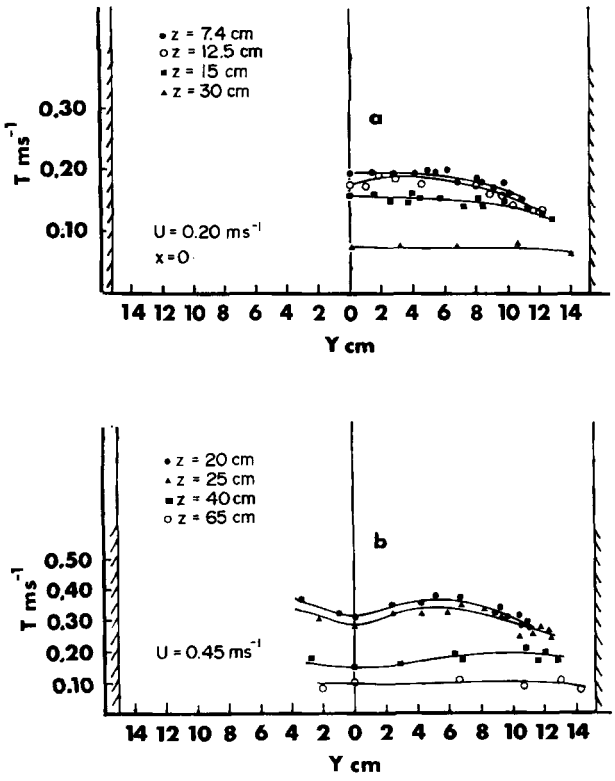

Figure 8. Horizontal distribution of RMS gas velocities along *y* axis ($x = 0$).
Bed depth, $H = 5.2$ cm.

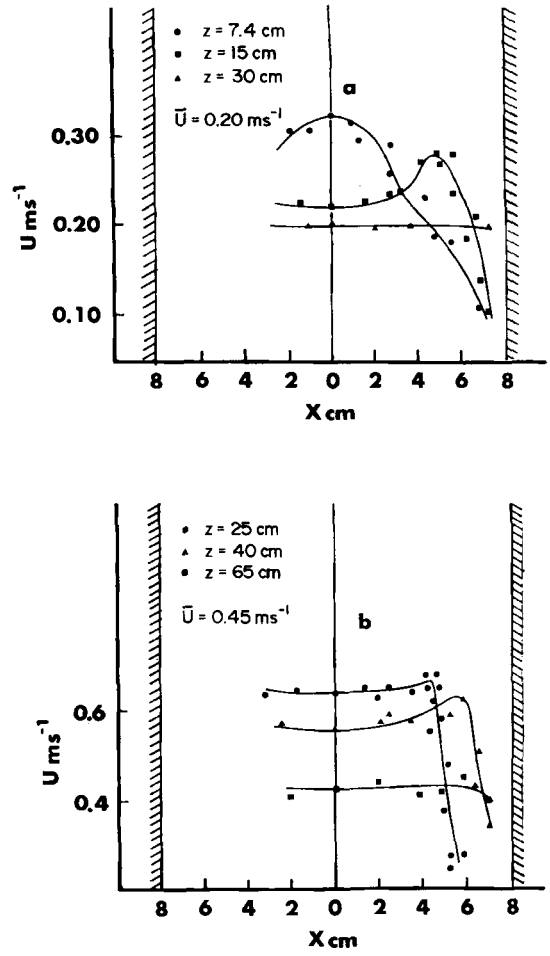

Figure 9. Horizontal distribution of local mean gas velocities along *x* axis ($y = 0$).
Bed depth, $H = 5.2$ cm.

turbulence value near the wall. At a sufficient freeboard height, it levels out and becomes equal to the free stream turbulence level.

Figure 9a shows the variation of gas velocity with the x direction (shorter axis) at $\bar{U} = 0.20$ ms^{-1} for three freeboard heights. The same kind of velocity profiles observed in Figure 7a can be seen for the short axis traverse.

The same kind of decay of the axial gas velocity profiles can be observed at fluidization velocity of 0.45 ms^{-1}, Figure 7b. From the figures it is observed that as the volumetric air flow increases, the axial velocity profiles become more flat; i.e., there is less decay.

The horizontal distribution of gas velocity in the freeboard shows a unique character that has not previously been reported. Although Levy and Lockwood (1983) reported a "crater" type distribution across the freeboard, they did not make measurements at low freeboard levels. From Figure 7a it is seen that at $z = 7.4$ cm, the maximum is on the centerline, indicating the migration of the bubbles toward the center as they move up in the dense bed.

Grace and Harrison (1968) reported that in a two-dimensional bed, assuming a uniform distribution of bubbles at the distributor, the bubbles move away from the wall because of coalescence. Werther and Moulerus (1973) found the same kind of bubble flow pattern in which bubbles systematically move to the center (and expand) with height.

This explains why the maximum velocity is located at the center. From Figure 7a ($z = 7.4$ cm) it is also seen that the bubble coalescence occurs not only at the center but also at locations close to the center. As the ghost bubbles move up in the freeboard this distinct character of the velocity profile is replaced by another unique profile. At $z = 12.5$ cm the slope of the velocity profile changes and the maxima shift close to the wall. The mechanism whereby this change in the velocity profile takes place is not fully understood. No information leading to an explanation for this abrupt change has been found in the literature.

Al Taweel and Landau (1978) suggested a model to predict the effect of particles on the turbulence structure of flowing gas-solid suspensions. They reported that the inability of particles to fully follow the turbulence fluctuations generates fluctuating relative velocities between the gas and particles, resulting in additional energy dissipation caused by shearing action between the phases. This may explain the change in the velocity profile. As the gas moves further up in the freeboard the wall shear stress becomes more effective; thus, the maximum moves back to the center.

Another plausible explanation is that the ghost bubbles break up as they rise in the freeboard, yielding smaller bubbles. Once the ghost bubbles break up, they will move to the wall by the dissipative eddies. The ghost bubble rise velocity at the bed surface is $U_{bro} = 0.711\ (gD_b)^{1/2}$. From the axial velocity profiles in

Figure 3a, it is seen that the ghost bubble velocity decays with freeboard height; thus, the ghost bubble diameter, D_b, must decrease with height.

Davidson and Harrison (1963) suggested that in a spherical-cap bubble there is an upward velocity along the centerline of magnitude of the order of U, and this is large enough to lift particles from the wake into the bubble, so causing the breakup of the bubble.

Effect of bed depth

Another set of experiments was conducted to measure the axial gas velocity distribution and turbulence intensity at a different static bed height. In these experiments the bed height was 12 cm. The results for three fluidizing velocities ($\bar{U}$ = 0.20, 0.28, and 0.40 ms^{-1}) are shown in Figure 10. At $\bar{U}$ = 0.20 ms^{-1} the centerline gas velocity increased with bed depth. For the fluidizing velocities 0.28 and 0.40 ms^{-1} the increase of the velocity was less. The variation of turbulence intensity with bed depth increased approximately by 35%, which corresponds to the value of bubble growth caused by the increase in bed depth. This confirms that turbulence in the freeboard is induced by the bubbles erupting at the center, and its level is strongly dependent on bubble size.

Theoretical

It is assumed that the bubbles breaking at the dense bed surface maintain their entities in the freeboard as suggested by

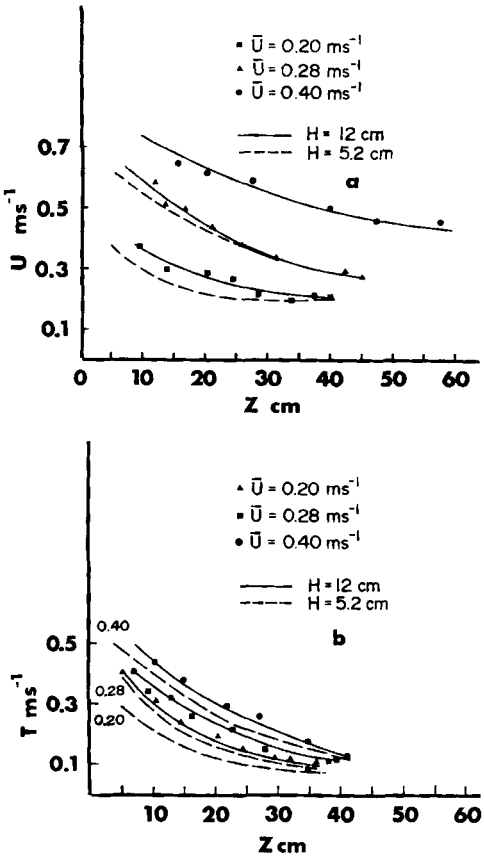

Figure 10. Effect of bed depth on local mean and RMS gas velocities.

Pemberton and Davidson (1984). Kehoe (1969) named these entities "ghost bubbles."

The bulk behavior of the gas in the freeboard can be determined from the collective effect of the motion of the ghost bubbles. The ghost bubbles in the freeboard behave like eddies/entities with extra momentum in the axial direction compared to the surrounding fluid. They lose the extra momentum as they move relative to the surrounding fluid, mainly from inertial drag because of their size and velocity. A similar mechanism for the decay of turbulent entities by viscous drag was proposed by Tyldesley and Silver (1968). They suggested that the entities keep their size and identity until the extra momentum is lost.

The deceleration of a ghost bubble by inertial drag with the freeboard height can be written by momentum balance as:

$$\frac{d(V_b \rho U_b)}{dt} = F_D \tag{1}$$

and the drag force acting on the bubble can be expressed as:

$$F_D = -C_D A_b \cdot \rho(U_b - \bar{U})^2/2 \tag{2}$$

where C_D is the drag coefficient.

As the ghost bubbles emerge at the bed surface with their ejection velocity, and maintain their entity in the freeboard, as an approximation it is further assumed that their rise velocity in the freeboard can be estimated from Davidson and Harrison's (1963) correlation for the rise velocity inside the dense bed, Pemberton (1982).

$$U_b = (\bar{U} - U_{mf}) + U_{br} \tag{3}$$

where U_{br} is the relative bubble velocity

$$U_{br} = 0.711\sqrt{gD_b} \tag{4}$$

and

$$\frac{dU_b}{dt} = \frac{dU_b}{dh} \cdot \frac{dh}{dt} = U_b \frac{dU_b}{dh} \tag{5}$$

Since the bubble (entity) is assumed to behave as a solid, the drag coefficient C_D can be considered a constant. Davidson and Harrison (1963) used C_D = 2.64 for an isolated bubble in an infinite medium. In the presence of multiple ghost bubbles emerging from the bed, the drag coefficient is calculated by the expression suggested by Ishii and Zuber (1979) as

$$C_D = \frac{8}{3}(1 - \alpha)^2 \tag{6}$$

where α is the void fraction of the ghost bubbles. The drag coefficient is taken as C_D = 0.44 for α_{max} = 0.6.

Combining Eqs. 1 through 6, rearranging and integrating with the boundary condition $U_{br} = U_{bro}$ at $h = 0$, yields

$$\frac{\bar{U}}{(U_{bro} - U_{mf})}\left(\frac{U_{bro} - U_{mf}}{U_{br} - U_{mf}} - 1\right) + \ln\frac{U_{bro} - U_{mf}}{U_{br} - U_{mf}} = \beta h \tag{7}$$

where

$$\beta = \frac{1}{3D_b} \tag{8}$$

and U_{bro} is the relative bubble velocity at the bed surface.

Pemberton and Davidson (1984) proposed a model to predict the motion of ghost bubbles in the freeboard. Their model is based on Maxworthy's (1972) model of vorticity diffusion and gives the bubble velocity in terms of height above the bed surface. Equation 7 is identical to the expression obtained by Pemberton and Davidson, with the exception that the turbulent decay coefficient is equal to $\frac{1}{3} D_b$.

The prediction of β compares well with the best fit values of β for the experimental data of Pemberton and Davidson (1984), Horio et al. (1980), and the present experimental data, as shown in Figure 11. The assumption made in using Eq. 3 for ghost bubble rise velocity can thus be taken to be reasonably valid. From the experimental information gained in this study, it appears that the gas flow in the freeboard can be predicted reasonably well by the suggested model. The vortex ring model based on Maxworthy's (1972) viscous entrainment mechanism underestimates the decay by an order of magnitude.

Transport disengagement height

A model was developed to predict the transport disengagement height (TDH) in the freeboard. Horio et al. defined TDH as the height at which mass transfer of solids from the particle ascending zone to the particle descending zone near the wall becomes negligible. They assumed that the mass transfer coefficient is proportional to the square of the velocity fluctuations. Based on this assumption, they suggested that TDH corresponds to a position where the fluctuating gas velocity decays by 95%,

$$\frac{T - T_\infty}{U_b} = 0.05$$

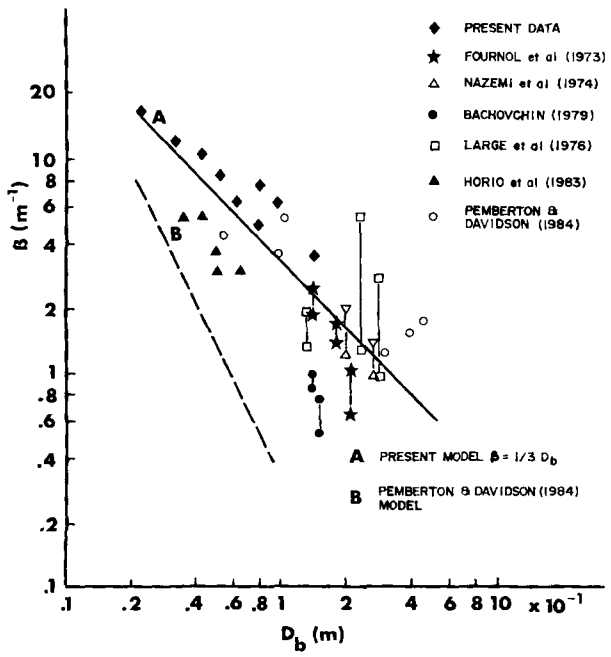

Figure 11. Log-log variation of turbulent decay constant vs. bubble diameter.

and obtained an equation for TDH as

$$\text{TDH} = 14(D_b/g)^{1/2} \tag{9}$$

In this study a similar mechanism for particle disengagement is assumed. Further, it is assumed that at the TDH the ghost bubble velocity becomes equal to the average gas velocity; i.e., the gas velocity fluctuations become constant.

Equation 7 can be rewritten as

$$\frac{U'}{U'_0} = e^{-\beta h + U/U_0(U_0/U' - 1)} \tag{10}$$

where

$$U'_0 = U_{bro} - U_{mf}$$
$$U' = U_{br} - U_{mf}$$

From Eq. 3, $U_g = \bar{U} - U_{mf} + U_{br}$ for

$$U_g \to \bar{U}$$
$$U_{br} - U_{mf} \to 0$$

thus

$$U' \to 0$$

Substituting the expression for $\beta = (1/3D_b)$, TDH is obtained as:

$$\text{TDH} \simeq 12D_b \tag{11}$$

From the regression analysis of the experimentally obtained TDH values, the following relation is obtained

$$\text{TDH} = 11.7D_b \tag{12}$$

The bubble diameter D_b was obtained from an expression given by Mori and Wen (1975). This shows that Eq. 11 predicts the TDH reasonably well (5%), Figure 12. The experimental TDH values were obtained by assuming that TDH is the position

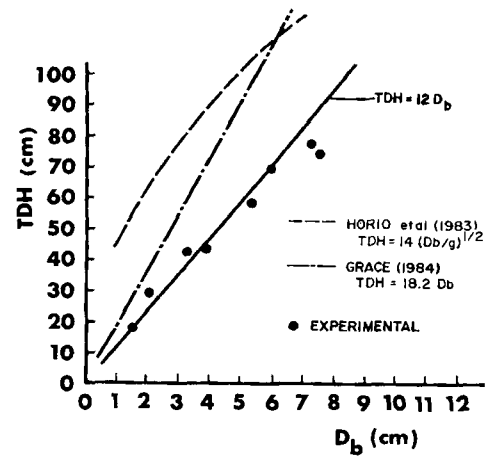

Figure 12. Comparison of experimental and predicted TDH values vs. bubble diameter.

where the local mean gas velocity becomes nearly equal to the superficial gas velocity.

Acknowledgment

The authors would like to thank the Natural Sciences and Engineering Research Council of Canada for its support of this project.

Notation

A_b = cross-sectional area of a bubble
C_D = drag coefficient
D_b = bubble diameter
F_D = drag force
g = acceleration of gravity
h = height above bed surface
T = RMS velocity $\sqrt{(\overline{U' - U})^2}$
T_∞ = RMS value in fully developed turbulence
t = time
U_b = bubble rise velocity
U = fluidizing velocity
U_{mf} = minimum fluidization velocity
U_{br} = relative bubble rise velocity
U_{bro} = relative bubble rise velocity at bed surface
U = gas velocity
V_b = volume of a ghost bubble
ρ = air density

Literature cited

Al Taweel, A. M., and J. Landau, "The Effect of Turbulence Modulation on the Rate of Heat Transfer to Gas-Solid Suspensions," *J. Eng. Sci.*, College of Eng., Univ. of Riyadh, **4**(2), 97 (1978).

Amyotte, P. R., and F. Hamdullahpur, "Technical University of Nova Scotia Laser Doppler Velocimetry System," Tech. Rep. No. TR-001, Halifax (1984).

Bachovchin, D. M., J. M. Beer, and A. F. Sarofim, "An Investigation into the Steady State Elutriation of Fines from a Fluidized Bed," AIChE 72nd Ann. Meet., San Francisco (1979).

Davidson, J. F., and D. Harrison, *Fluidized Particles*, Cambridge Univ. Press (1963).

Do, H. T., J. R. Grace, and R. Clift, "Particle Ejection and Entrainment from Fluidized Beds," *Powder Technol.*, **6**, 195 (1972).

Fournol, A. B., M. A. Bergougnou, and C. G. T. Baker, "Solids Entrainment in a Large Gas-Fluidized Bed," *Can. J. Chem. Eng.*, **51**, (1973).

Grace, J. R., and D. Harrison, "The Distribution of Bubbles within a Gas-Fluidized Bed," *Inst. Chem. Eng. Symp. Ser.*, **30**, 105 (1968).

Hamdullahpur, F., "Two-Phase Flow Behavior in the Freeboard of a Gas-Fluidized Bed," Ph.D. Diss. Tech. Univ. Nova Scotia, Halifax (1985).

Horio, M., A. Taki, Y. S. Hsieh, and I. Muchi, "Elutriation and Particle Transport through the Freeboard of a Gas-Solid Fluidized Bed," *Fluidization*, J. R. Grace and J. M. Matsen, eds., Plenum, New York (1980).

Ishii, M., and N. Zuber, "Drag Coefficient and Relative Velocity in Bubbly, Droplet, or Particulate Flows," *AIChE J.*, **22**, 843 (1979).

Keohe, P. W. K., "The Effect of Particle Size on Slugging Fluidized Bed," Ph.D. Diss., Univ. Cambridge (1969).

Large, J. F., Y. Martine, and M. A. Bergougnou, "Interpretative Model for Entrainment in a Large Gas-Fluidized Bed," Int. Powder Bulk Solids Handling, Processing Conf., *J. Bulk Solids Technol.*, 15-21 (1976).

Levy, Y., and F. Lockwood, "Laser Doppler Measurements of Flow in Freeboard of a Fluidized Bed," *AIChE J.*, **29**(6), 889 (1983).

Maxworthy, T., "The Structure and Stability of Vortex Rings," *J. Fluid Mech.*, **51**(1) (1972).

Mori, S., and C. Y. Wen, "Estimation of Bubble Diameter in Gaseous Fluidized Beds," *AIChE J.*, **21**(7), (Jan., 1975).

Morooka, S., T. Kago, and Y. Kuto, "Flow Pattern of Solid Particles in Freeboard of Fluidized Bed," *Proc. 4th Int. Conf. Fluidization*, Japan (1983).

Nazemi, A., M. A. Bergougnou, and C. G. J. Baker, "Dilute Phase Holdup in a Large Gas-Fluidized Bed," *AIChE Symp. Ser. No. 141*, **70** (1974).

Parker, C. A., *Photoluminescence of Solutions*, Elsevier, Amsterdam (1968).

Pemberton, S. T., "Entrainment from Fluidized Beds," Ph.D. Diss., Cambridge Univ. (1982).

Pemberton, S. T., and J. F. Davidson, "Turbulence in the Freeboard of a Gas-Fluidized Bed," *Chem. Eng. Sci.*, **39**(5), 829 (1984).

Stevenson, W. H., R. dos Santos, and S. C. Mettler, "A Laser Velocimetry Utilizing Laser-Induced Fluorescence," *App. Phys. Lett.*, **27**(7), 395 (1975).

Tyldesly, J. R., and R. S. Silver, "The Prediction of the Turbulent Properties of a Turbulent Fluid," *Int. J. Heat Mass Trans.*, **11**, 1325 (1968).

Werther, J., and O. Molerus, "The Local Structure of Gas-Fluidized Beds. II: The Spatial Distribution of Bubbles," *Int. J. Multiph. Flow*, **1**, 123 (1973).

Manuscript received Feb. 4, 1986, and revision received June 9, 1986.